

- [11] R. A. Segalman, H. Yokoyama, E. J. Kramer, *Adv. Mater.* **2001**, *13*, 1152.
- [12] M. Trawick, D. Angelescu, P. Chaikin, J. Sebastian, R. Register, D. Adamson, C. Harrison, *Bull. Am. Phys. Soc.* **2002**, *47*, 970.
- [13] C. Park, C. De Rosa, E. L. Thomas, *Macromolecules* **2001**, *34*, 2602.
- [14] L. Rockford, Y. Liu, P. Mansky, T. P. Russell, M. Yoon, S. G. J. Mochrice, *Phys. Rev. Lett.* **1999**, *82*, 2602.
- [15] S. O. Kim, H. H. Solak, M. P. Stoykovich, N. J. Ferrier, J. J. de Pablo, P. F. Nealey, *Nature* **2003**, *424*, 411.
- [16] A. Keller, E. Pedemonte, F. M. Willmouth, *Nature* **1970**, *225*, 538.
- [17] G. Hadziioannou, A. Mathis, A. Skoulios, *Colloid Polym. Sci.* **1979**, *257*, 136.
- [18] M. Kimura, M. J. Misner, T. Xu, S. H. Kim, and T. P. Russell, *Langmuir* **2003**, *19*, 9910.
- [19] J. M. Sebastian, C. Lai, W. W. Graessley, R. A. Register, *Macromolecules* **2002**, *35*, 2707.
- [20] C. Harrison, Z. Cheng, S. Sethuraman, D. Huse, P. M. Chaikin, D. A. Vega, J. M. Sebastian, R. A. Register, D. H. Adamson, *Phys. Rev. E* **2002**, *66*, 011706.
- [21] N. P. Balsara, H. J. Dai, *J. Chem. Phys.* **1996**, *105*, 2942.
- [22] P. M. Chaikin, T. C. Lubensky, *Principles of Condensed Matter Physics*, Cambridge University Press, Cambridge, UK **1995**.
- [23] I. W. Hamley, *Macromol. Theory Simul.* **2000**, *9*, 363.
- [24] M. Bahiana, Y. Oono, *Phys. Rev. A* **1990**, *41*, 6763.
- [25] D. E. Angelescu, *Ph. D. Thesis*, Princeton University, **2003**.
- [26] S. R. Ren, I. W. Hamley, *Phys. Rev. E* **2001**, *63*, 041503.
- [27] M. W. Hamersky, M. Tirrell, T. P. Lodge, *Langmuir* **1998**, *14*, 6974.
- [28] M. C. Dalvi, C. E. Eastman, T. P. Lodge, *Phys. Rev. Lett.* **1993**, *71*, 2591.
- [29] C. E. Eastman, T. P. Lodge, *Macromolecules* **1993**, *27*, 5591.
- [30] J. C. Meredith, A. P. Smith, A. Karim, E. J. Amis, *Macromolecules* **2000**, *33*, 9747.

Self-Catalysis and Phase Transformation in the Formation of CdSe Nanosaws**

By Yong Ding, Christopher Ma, and Zhong Lin Wang*

Wurtzite-structured CdSe is an important type II–V semiconducting compound for optoelectronics.^[1,2] Due to the high precision of size controllability, CdSe quantum dots are the most extensively studied quantum nanostructure, and they have been used as a model system for investigating a wide range of nanoscale electronic, optical, optoelectronic, and chemical processes.^[3,4] Although studies of CdSe have been carried out for more than a dozen years, there are only a few reports on the synthesis of quasi-one-dimensional CdSe nano-

structures. Shape-controlled synthesis of CdSe nanorods,^[5,6] and template-assisted synthesis of CdSe nanowires^[7] and nanotubes^[8] have been demonstrated using electrochemical and chemical approaches. Two-dimensional arrays of CdSe pillars have been fabricated using electron-beam lithography.^[9] These nanowires and nanotubes are composed of nanometer-sized grains, and are polycrystalline in nature. Recently, we reported a single-crystal nanobelt/nanoribbon structure of wurtzite CdSe, parts of which display a “saw” shape.^[10]

In this communication, a detailed structural analysis of the formation process of CdSe nanosheets and nanosaws is presented. The CdSe nanostructures have an identical growth direction of $[01\bar{1}0]$, and top and bottom surface planes of $(2\bar{1}10)$ across a large temperature zone. The growth of the special tooth-shaped saw structure is suggested to be a combined result of secondary epitaxial-nucleation processes owing to zinc-blende–wurtzite phase transformations and to the self-catalytic effect of the Cd-terminated (0001) surface.^[11,12]

The CdSe nanobelts were synthesized by a thermal-evaporation process in a horizontal-tube furnace.^[10] The as-synthesized samples were first analyzed by scanning electron microscopy (SEM) to find the relationship between the deposition temperature and their growth morphologies. The SEM images of the samples collected in low-temperature ($\sim 600^\circ\text{C}$) and high-temperature ($\sim 700^\circ\text{C}$) regions are shown in Figures 1a,b, respectively. The plot in Figure 1c depicts the relationship between the local substrate temperature and the distance from the center of the furnace. The length of the silicon substrate used in our experiment is around 10 cm and its position in the furnace is illustrated in Figure 1c. The SEM images in Figures 1a,b were obtained from the regions marked a and b in Figure 1c, corresponding to temperatures of ~ 600 and $\sim 700^\circ\text{C}$, respectively. The SEM images reveal that the samples in the lower and higher temperature regions show nanobelt/nanosheet and nanosaw structures, respectively.

The structures of the nanobelts/nanosheets and nanosaws have been analyzed to understand the temperature dependence of the growth morphology. Figure 2a is a low-magnification transmission electron microscopy (TEM) image of a nanobelt/nanosheet collected in the lower-temperature region. The length and width are hundreds and several micrometers, respectively, while the thickness of the nanobelt is no more than 20 nm, as indicated by the bending area of the belt, which has a typical sheet morphology. The selected area electron diffraction (SAED) pattern (Fig. 2a, inset) indicates that the nanobelt/nanosheet has a wurtzite structure, and grows along $[01\bar{1}0]$. After examining more than fifty belts from the same temperature region, only one of them grows along $[0001]$, while the remaining ones grow along $[01\bar{1}0]$. High-resolution TEM (HRTEM) imaging confirms the growth direction of the belt (Fig. 2b). Despite the uniform thickness of the belt, the surfaces on either side are not parallel to each other. The surface on one side is the perfect (0001) plane, but the surface on the other side has steps, indicating asymmetric surface activities on the Cd-terminated (0001) and Se-terminated $(000\bar{1})$ surfaces, analogous to the case of ZnO.^[11]

[*] Prof. Z. L. Wang, Dr. Y. Ding, C. Ma
School of Materials Science and Engineering
Georgia Institute of Technology
Atlanta, GA 30332-0245 (USA)
E-mail: zhong.wang@mse.gatech.edu

[**] Thanks to the financial support from the US NSF NIRT ECS-0210332. Thanks to Daniel Moore for calibrating the furnace.

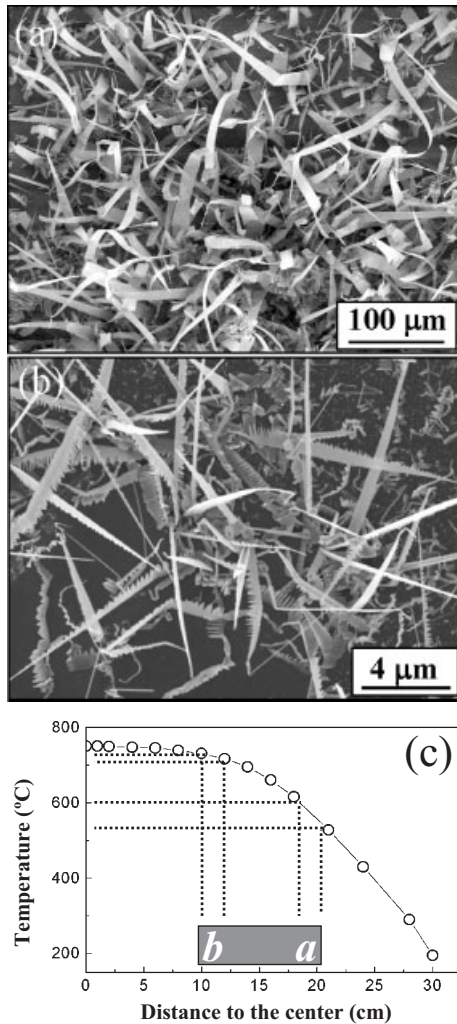


Figure 1. a,b) SEM images show a) nanosheet/nanobelt and b) nanosaw morphologies, corresponding to $\sim 600^\circ\text{C}$ and 700°C substrate temperatures, respectively. c) Plot shows the relationship between the local temperature on the substrate, shown in grey, and the distance from the center of the furnace.

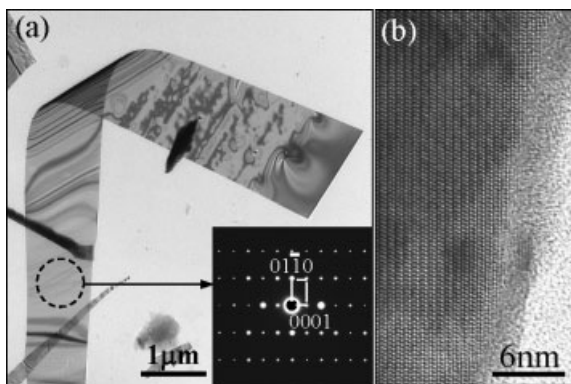


Figure 2. a) Low-magnification TEM image of a nanosheet collected in the low temperature region. The SAED pattern (insert) was recorded from the circled area. b) HRTEM image of the surface of one side of the belt.

Figure 3a is a typical TEM image obtained from the front section of a nanosaw structure collected in the higher-temperature region, showing asymmetric growth behavior. The Au catalyst can be seen at the tip of the nanosaw. The Au

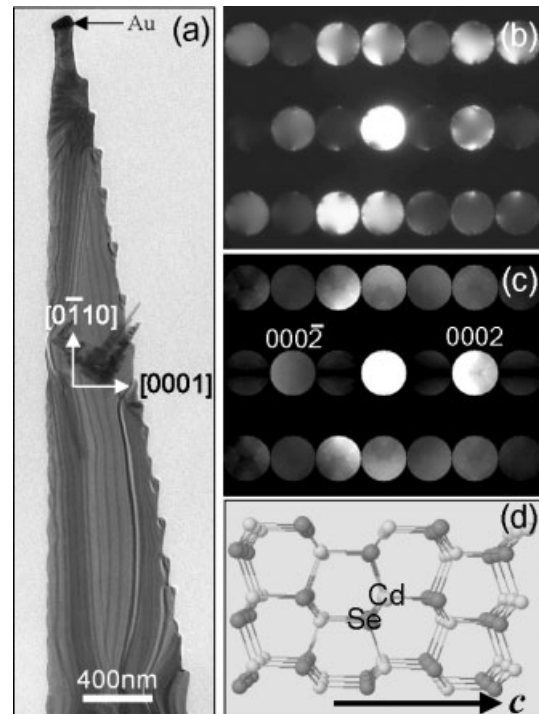


Figure 3. a) A TEM image showing the front section of a CdSe nanosaw. b) Experimental and c) simulated CBED patterns. d) Atomic model of the wurtzite-structured CdSe.

gent-beam electron diffraction (CBED) pattern recorded from the saw in Figure 3a is shown in Figure 3b. By combining the CBED pattern and the bright-field TEM image, the structure of the nanosaw is defined. The dominant growth direction of the ribbon is $[0\bar{1}10]$ and the large top and bottom surfaces are $\pm(2\bar{1}\bar{1}0)$, which are the same as the belts collected in the low-temperature region. Because wurtzite has a non-central symmetry, CBED may be applied to determine the polarity along $[0001]$ if the sample is sufficiently thick to create a strong dynamic diffraction.

In order to differentiate the Cd-terminated (0001) surface from the Se-terminated $(000\bar{1})$ surface in the wurtzite structure, the $[2\bar{1}\bar{1}0]$ zone-axis CBED patterns with different sample thicknesses were simulated to compare with the experimental data presented in Figure 3b.^[13] The best-matched simulated image is shown in Figure 3c, which corresponds to a sample thickness of 19 nm. The qualitative agreement between the calculated and simulated data suggests that the nanoteeth are located along Cd-terminated $[0001]$.

It has been reported that self-catalysis at the Zn-terminated (0001) surface of ZnO results in the growth of aligned nanocantilever arrays, but the O-terminated $(000\bar{1})$ surface is inert.^[11] The atomic model of wurtzite-structured CdSe is de-

pictured in Figure 3d. The Cd-terminated and Se-terminated planes compose the (0001) and (000 $\bar{1}$) planes, respectively. The CdSe saw structure shown in Figure 3a could also be due to self-catalysis at the Cd-terminated (0001) surface, while the Se-terminated (000 $\bar{1}$) surface could be inactive, resulting in the asymmetric growth morphology.

Figures 4a,b are typical TEM images obtained from the main part of the nanosaw structures collected from the high-temperature region, which also show asymmetric growth

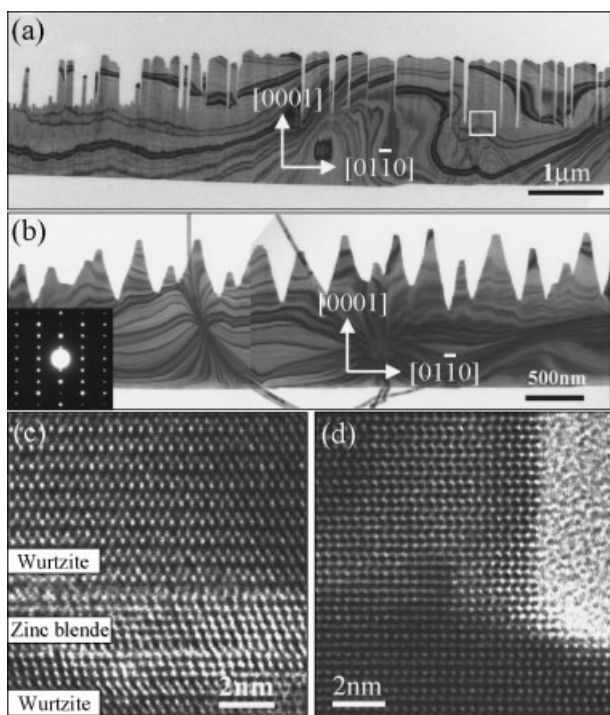


Figure 4. a,b) TEM images of the asymmetric growth behavior of the nanosaw structures, with SAED pattern (b, insert). c) HRTEM image recorded from the rectangle-enclosed area in (a) showing the existence of zinc-blende structure. d) The HRTEM image from the zigzag region in (c) shows neither planar defects nor a zinc-blende phase.

behavior. One side is flat, but the other side has teeth (Fig. 4a) or zigzag shapes (Fig. 4b). The strong diffraction contrast observed in the images is due to the high-quality single-crystal structure of the nanosaw. A HRTEM image collected near the root of the nanoteeth indicates the existence of a different phase, which is several atomic layers in thickness and corresponds to the zinc-blende-structured CdSe (Fig. 4c). The zinc blende is a result of changing the stacking sequence from ABAB for the hexagonally structured wurtzite to ABCABC. The energies for the two phases are quite close,^[14] and it is relatively easy to stimulate phase transformation. An analogous structure has been previously reported for ZnS.^[15] The magnitude in morphology oscillation for the zigzag structure is much smaller than that for the nanoteeth. HRTEM images obtained from the zigzag region reveal neither planar defects nor a zinc-blende phase (Fig. 4d).

The formation of the one-sided saw and zigzag structures may be due to two factors. First, it could be due to the self-catalyzed processes at the Cd-terminated (0001) surface which result in the asymmetric growth morphology. Second, the nanoteeth growing along [0001] are straight, with well-defined shapes. The growth of the side nanoteeth may also be related to the presence of the zinc-blende layer. From the structural information shown in Figures 4a,b, the top and bottom surfaces of the wurtzite phase are the $\pm(2\bar{1}10)$ low-energy facets. However, the corresponding planes for the zinc-blende phase are $\pm(110)$, which are the high-energy facets for the cubic system and are thus energetically unfavorable. Therefore, the width of the zinc-blende strip is limited in order to reduce its surface energy, but continuous growth driven by the catalytically active Cd-terminated (0001) surface tends to re-nucleate the wurtzite phase. This nucleation is epitaxial, but multiple nucleation sites along the length of the nanoribbon are most likely, possibly resulting in the growth of the nanoteeth on one side. The uneven growth of the nanoteeth can be clearly seen on the right-hand side of the nanosaw shown in Figure 3a.

It has been noted that the non-even lengths of the nanoteeth shown in Figure 3a may be due to differences in growth time. The growth is a two-step process: a Au-catalyzed fast-growth process creates the nanoribbon, while a slower side-growth process creates the teeth. As the Au-catalyzed growth continues along [01 $\bar{1}0$], the self-catalyzed growth proceeds simultaneously along [0001]. The local growth temperature may greatly affect the rate of the self-catalyzed growth, resulting in the formation of nanosaws in a higher-temperature region, but nanobelts/nanosheets in a lower-temperature region (see Fig. 1).

In summary, wurtzite-structured CdSe nanobelts/nanosheets and nanosaws have been synthesized by a thermal-evaporation process using a Au catalyst. The CdSe nanostructures have an identical growth direction of [01 $\bar{1}0$], and top and bottom flat surfaces of (2 $\bar{1}10$). The comparably low deposition temperature ($\sim 600^\circ\text{C}$) benefits the formation of pure wurtzite-phase nanobelts/nanosheets. A detailed structural analysis on the formation process of wurtzite CdSe nanosheets and nanosaws is presented. The nanosaw is formed by a two-step process: a fast-growth process along [01 $\bar{1}0$] creates the main ribbon, while a subsequent side-growth process along [0001] creates the one-sided teeth. The growth of the teeth is suggested to result from a combination of secondary epitaxial nucleation processes due to zinc-blende–wurtzite phase transformations, and to the self-catalytic effect of the Cd-terminated (0001) surface.

Experimental

The CdSe nanobelts were synthesized through a thermal-evaporation process in a horizontal-tube furnace. Commercial-grade CdSe powder was placed in the center of a single-zone tube furnace and evacuated for several hours to purge oxygen from the chamber. Single-crystal silicon substrates, dispersed with catalytic gold particles

typically 3–5 nm in size, were used for growing the nanostructures. After the evacuation process was completed, the temperature of the system was elevated to 750 °C at a rate of 20 °C min⁻¹ and the pressure was maintained at 30 kPa. Nitrogen was sent through the system at a rate of 50 mL min⁻¹ to act as a carrier gas to transport the sublimated vapor to cooler regions within the tube furnace for deposition. The as-produced materials were analyzed by scanning electron microscopy and high-resolution transmission electron microscopy.

Received: March 8, 2004
Final version: July 2, 2004

- [1] G. Hodes, A. Albu-Yaron, F. Decker, P. Motisuke, *Phys. Rev. B* **1987**, 36, 4215.
- [2] M. Ichimura, N. Sato, A. Nakamura, K. Takeuchi, E. Arai, *Phys. Status Solidi A* **2002**, 193, 132.
- [3] S. H. Tolbert, A. P. Alivisatos, *Science* **1994**, 265, 373.
- [4] M. G. Bawendi, A. R. Kortan, M. L. Steigerwald, L. E. Brus, *J. Chem. Phys.* **1989**, 91, 7282.
- [5] X. G. Peng, L. Manna, W. D. Yang, J. Wickham, E. Scher, A. Kadavanich, A. P. Alivisatos, *Nature* **2000**, 404, 59.
- [6] J. T. Hu, L. S. Li, W. D. Yang, L. Manna, L. W. Wang, A. P. Alivisatos, *Science* **2001**, 292, 2060.
- [7] X. S. Peng, J. Zhang, X. F. Wang, Y. W. Wang, L. X. Zhao, G. W. Meng, L. D. Zhang, *Chem. Phys. Lett.* **2001**, 343, 470.
- [8] X. C. Jiang, B. Mayers, T. Herricks, Y. N. Xia, *Adv. Mater.* **2003**, 15, 1740.
- [9] Y. W. Wu, C. S. Wu, C. C. Chen, C. D. Chen, *Adv. Mater.* **2003**, 15, 49.
- [10] C. Ma, Y. Ding, D. Moore, X. D. Wang, Z. L. Wang, *J. Am. Chem. Soc.* **2004**, 126, 708.
- [11] Z. L. Wang, X. Y. Kong, J. M. Zuo, *Phys. Rev. Lett.* **2003**, 91, 185502.
- [12] E. A. Stach, P. J. Pauzauskie, T. Kuykendall, J. Goldberger, R. He, P. Yang, *Nano Lett.* **2003**, 3, 867.
- [13] J. M. Zuo, J. C. Mabon, WebEMAPS software, University of Illinois at Urbana-Champaign; URL: <http://emaps.mrl.uiuc.edu/>
- [14] C. Y. Yeh, Z. W. Lu, S. Froyen, A. Zunger, *Phys. Rev. B* **1992**, 46, 10086.
- [15] C. Ma, D. Moore, J. Li, Z. L. Wang, *Adv. Mater.* **2003**, 15, 228.

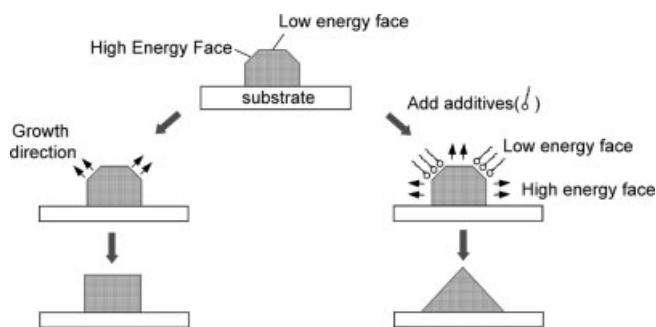
Electrochemical Crystallization of Cuprous Oxide with Systematic Shape Evolution**

By Matthew J. Siegfried and Kyoung-Shin Choi*

The shape of a crystal is determined by the crystallographic planes that form the surface. The density and symmetry of atoms in different crystallographic planes are not identical,

and neither are their electronic structure, bonding, surface energy, and chemical reactivities. Therefore, the ability to tune the shapes of materials directly relates to the ability to tune their properties and stabilities. While many successful attempts have been reported to manipulate the shape of isolated inorganic particles,^[1–5] it remains a challenge to systematically modify the shape of particles that are composed of polycrystalline films, or electrode materials. A synthetic method that possesses such an ability is critical to elucidate any shape-dependence of chemical and physical properties. It will also generate many possibilities of improving the efficiency of devices based on semiconducting/metallic electrodes (e.g., photovoltaics, fuel cells, sensors, and battery applications). In this study, we demonstrate a synthetic method that can precisely and homogeneously control the shape of micrometer-size cuprous oxide (Cu₂O) crystals grown onto a conducting substrate.

When inorganic crystals are formed under equilibrium conditions, their crystal habit is determined by the relative order of surface energies.^[6] The fastest crystal growth will occur in the direction perpendicular to the face with the highest surface energy. This results in the elimination of higher-energy surfaces while the lower-energy surfaces increase in area. When organic or inorganic additives are added during the crystal growth process, the relative order of surface energies can be modified.^[7] Due to anisotropy in adsorption stability, these additives adsorb onto a certain crystallographic plane more strongly than others. This preferential adsorption lowers the surface energy of the bound plane and hinders the crystal growth perpendicular to this plane, resulting in a change in the final morphology (as depicted in Scheme 1).



Scheme 1. Crystal-habit control achieved by preferential adsorption of additives during the crystal growth process.

We are interested in combining this concept with an electro-deposition method in order to produce semiconducting materials as polycrystalline electrodes with a precisely controlled morphology. Although it has been widely accepted that additives in plating solutions generally modify the surface features of inorganic deposits,^[8] not many systematic attempts have been made to investigate preferential adsorption of additives to methodically tune particle shapes. Our interest lies specifically in utilizing surfactant molecules as additives instead of simple inorganic ions^[9] or organic molecules.^[10] Due to their

*] Prof. K.-S. Choi, M. J. Siegfried
Department of Chemistry
Purdue University
West Lafayette, IN 47907 (USA)
E-mail: kchoi1@purdue.edu

**] This work made use of the Life Science Microscopy Facility at Purdue University. We thank Ms. Debbie Sherman for her help with the scanning electron microscope.